

# 3-D PARTICLE-IN-CELL SIMULATIONS FOR QUASI-PHASE MATCHED DIRECT LASER ELECTRON ACCELERATION IN DENSITY-MODULATED PLASMA WAVEGUIDES \*

M.-W. Lin and I. Jovanovic<sup>†</sup>, Department of Mechanical and Nuclear Engineering,  
 The Pennsylvania State University, University Park, PA 16802, USA

## Abstract

Quasi-phase matched direct laser acceleration (DLA) of electrons can be realized with guided, radially polarized laser pulses in density-modulated plasma waveguides. A 3-D particle-in-cell simulation model has been developed to study the scheme in which an electron bunch from a laser wakefield accelerator is injected into a plasma waveguide for the second-stage DLA to higher energies. In addition to being driven directly by the laser field, the electrons also experience the laser pondermotive force and the electrostatic force from the excited plasma waves. The results lead to better understanding of the interactions among the electron bunch, the laser pulse and the background plasma. Selected bunch lengths, bunch sizes and time delays with respect to the laser pulse are assigned to the injected electrons in a series of simulations. The energy spectrum and emittance of the accelerated electron bunch vary depending on those initial conditions, and they can be chosen to optimize the DLA performance.

## INTRODUCTION

The limitations on the accelerating field amplitude in radio-frequency accelerators motivate the development of laser-based accelerator technologies with much greater acceleration gradients. Guiding a radially polarized laser pulse in a plasma waveguide has been proposed for realizing direct laser acceleration (DLA), in which the co-propagating electrons are accelerated by the axial electric field of the laser pulse [1]. The plasma waveguide extends the acceleration distance and provides the condition for quasi-phase-matching (QPM) between the accelerated electrons and the laser field for a net gain accumulation [2].

To improve the fidelity of the DLA simulation, particle-in-cell (PIC) simulations are developed for detailed studies of DLA with closed-loop solutions for the variation of the electromagnetic field and the dynamics of charged particles for the injected bunch and the background plasma. For DLA realized in a plasma waveguide, the electron bunch interacts with the electromagnetic field of a co-propagating laser pulse, but also with the electric field originating from the plasma density perturbation driven by the bunch charge and the laser pondermotive force. The goal of this work is to understand how the initial parameters of the injected bunch can be chosen to optimize the DLA. Selected time delays (with respect to the laser pulse), bunch lengths, and

bunch sizes are assigned to the injected electrons in a series of simulations. We analyze the energy spectrum, trace space, emittance, and electron density distribution to understand the variation of bunch properties throughout the DLA process and how they relate to the initial conditions.

## THE 3-D PIC MODEL

A PIC model has been developed using the framework of the commercial software package VORPAL [3], in which a 3-D Cartesian coordinate system ( $x, y, z$ ) is defined and the laser pulse propagates along the  $x$ -axis. The size of the simulation box is  $L_x = 23.38 \mu\text{m}$  in the axial  $x$  direction and  $L_y \times L_z = 60 \mu\text{m} \times 60 \mu\text{m}$  in the transverse directions  $y$  and  $z$ . Each simulation has been performed in a moving frame co-propagating with the laser pulse at a speed of light in vacuum  $c$ . Fig. 1 summarizes the definition of the laser pulse for driving DLA and the plasma waveguide composed of alternating waveguide and neutral hydrogen sections, providing the necessary QPM condition. A 6-fs, 40-MeV bi-Gaussian

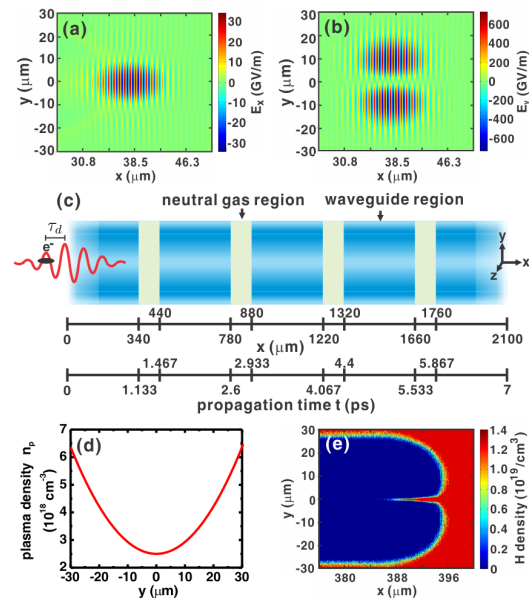


Figure 1: Snapshots of (a) axial  $E_x$  and (b) transverse  $E_y$  electric fields of a 20-fs, 0.5-TW, radially polarized laser pulse with a diameter  $w_D = 15 \mu\text{m}$ ; (c) illustration of a density-modulated plasma waveguide, along with the axial position  $x$  and the bunch propagation time  $t$ ; (d) transverse plasma density profile defined for the waveguide regions; (e) ionization of neutral hydrogen gas by the electric field in (a) and (b).

\* Work supported by the Defense Threat Reduction Agency.

<sup>†</sup> ijovanovic@psu.edu

Content from this work may be used under the terms of the CC BY 3.0 licence (© 2014). Any distribution of this work must maintain attribution to the author(s), title of the work, publisher, and DOI.

(having transverse and longitudinal Gaussian shapes) electron bunch with a diameter  $w_b = 3 \mu\text{m}$ , bunch charge of  $q_b = 5 \text{ pC}$ , and the peak density  $n_{b0} = 1.6 \times 10^{18} \text{ cm}^{-3}$  are chosen as the default bunch parameters for the simulation. Those parameters are typical for laser wakefield accelerated electrons. The initial energy spectrum for bunch electrons exhibits an energy spread of 4 MeV with an average energy  $T_0 = 40 \text{ MeV}$ . The default RMS normalized emittance in  $y$ -dimension is calculated as  $\epsilon_{N,y} \approx 1 \pi \text{ mm-mrad}$  by the definition :

$$\epsilon_{N,y} = \frac{4}{m_e c} \sqrt{\langle y^2 \rangle \langle P_y^2 \rangle - \langle y P_y \rangle^2} \pi \text{ mm-mrad}, \quad (1)$$

utilizing the particle positions  $y$  and momenta  $P_y$ .

## SIMULATION RESULTS

The injection delay  $\tau_d$  is defined here as the time delay between the peak of laser pulse envelope and the peak of the electron bunch density distribution. As shown in Fig. 2 (a), 6-fs long bunches injected with  $\tau_d = 6.2 \text{ fs}$ ,  $3.2 \text{ fs}$ ,  $0$ , and  $-3.2 \text{ fs}$  have an overall tendency to diverge and their emittance  $\epsilon_{N,y}$  values continue to increase in the propagation. Reducing the  $\tau_d$  helps to mitigate the bunch divergence for a smaller final value  $\epsilon_{N,y}$ , which corresponds to the less scattered particles around  $y = \pm 10 \mu\text{m}$  in the final trace space distributions shown in Fig. 2(b) with a decreased  $\tau_d$ . The improved collimation of the bunch with a smaller delay  $\tau_d$  can also be observed from the comparison of the particle

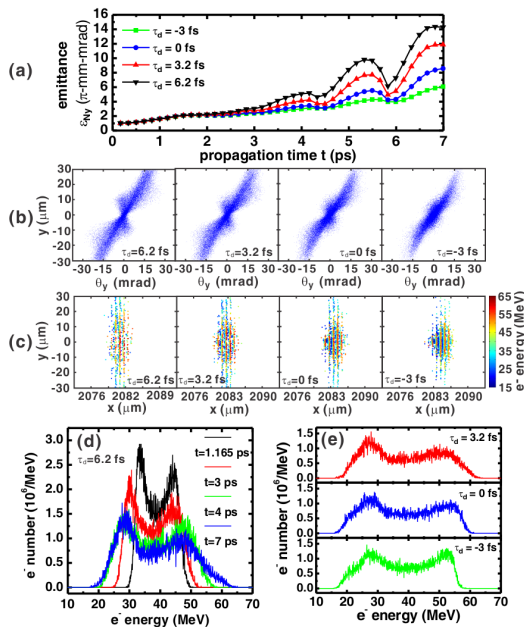


Figure 2: (a) Bunch emittance  $\epsilon_{N,y}$  as a function of the propagation time  $t$  for different time delays  $\tau_d = 6.2 \text{ fs}$ ,  $3.2 \text{ fs}$ ,  $0$ , and  $-3.2 \text{ fs}$ . Comparison for the final (b) trace space and (c) electron distributions. (d) Sampled variation of the energy spectrum  $\tau_d = 6.2 \text{ fs}$ . (e) Final energy spectra for  $\tau_d = 3.2 \text{ fs}$ ,  $0$ , and  $-3.2 \text{ fs}$ .

distributions in Fig. 2(c). Electrons are accelerated or decelerated in the DLA process depending on their axial injection phase, which results in the gradual broadening of the energy spectrum as illustrated in Fig. 2(d) for the bunch injected with  $\tau_d = 6.2 \text{ fs}$ . The radial Lorentz force  $F_r \propto q_e E_r$  also focuses or defocuses the bunch electrons according to their injection phases with respect to the radial field  $E_r$  [2]. Since the axial and radial field are out of phase by  $\pi/2$ , off-axis electrons injected near the optimal axial acceleration phases predominantly remain in the defocusing phases in the QPM process. Many of those electrons thus move to the outer radial region and, as a result, the electron number at the high-energy end of the final spectrum in Fig. 2(d) is significantly reduced. With a reduced  $\tau_d$ , the comparison of final electron energy spectra in Fig. 2(e) indicates an increased electron number in the range  $50 - 60 \text{ MeV}$  that is attributed to the reduced bunch divergence. However, the maximum energy in the spectrum drops from  $65 \text{ MeV}$  when  $\tau_d = 6.2 \text{ fs}$  to  $55 \text{ MeV}$  when  $\tau_d = -3.2 \text{ fs}$ , which is attributed to a decreased laser field amplitude the electrons experience in the acceleration process. Results presented here indicate a trend of increasing divergence in DLA of short electron bunches; the radial Lorentz force predominately drives the change of bunch emittance  $\epsilon_{N,y}$  throughout the process.

With a fixed injection delay  $\tau_d = 0$  and bunch charge of  $q_b = 5 \text{ pC}$ , Fig. 3(a) shows the comparison of on-axis plasma density  $n_{pe}(x)$  when bunch duration is set to  $\tau_b = 6 \text{ fs}$ ,  $13 \text{ fs}$  and  $20 \text{ fs}$ , while the rest of the bunch and laser

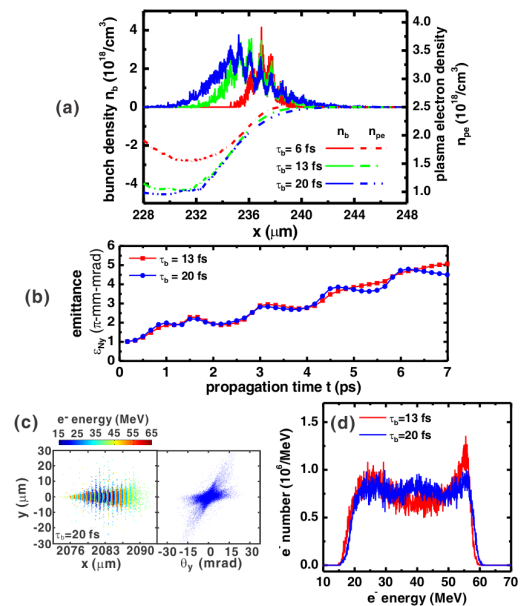


Figure 3: Comparison of the on-axis bunch density  $n_b$  and plasma electron density  $n_{pe}$  at  $t = 0.832 \text{ ps}$  for bunches with durations  $\tau_b = 6 \text{ fs}$ ,  $13 \text{ fs}$  and  $20 \text{ fs}$  are injected at  $\tau_d = 0$ . (b) Bunch emittance  $\epsilon_{N,y}$  as a function of propagation time  $t$  for bunches with durations  $\tau_b = 13 \text{ fs}$  and  $20 \text{ fs}$ . (c) Final trace space and electron distributions for  $\tau_b = 20 \text{ fs}$ . (d) Final energy spectra for  $\tau_b = 13 \text{ fs}$  and  $20 \text{ fs}$ .

parameters are kept the same as in the previous analysis. Regardless of the bunch duration  $\tau_b$ , the reduction of the plasma electron density  $n_{pe}(x)$  is always initiated at the leading edge of the bunch. For the 6-fs electron bunch having a length  $L_b = \tau_b c = 1.8 \mu\text{m}$ , the majority of bunch electrons do not experience a strong focusing force from the created ion channel since the variation of  $n_{pe}(x)$  is of order  $\lambda_p/4 = \pi c/2\omega_{p0} \approx 5.3 \mu\text{m}$  for the trailing edge. Therefore, for increased durations of the electron bunch of  $\tau_b = 13$  fs and 20 fs, the corresponding bunch lengths  $L_b = 3.9 \mu\text{m}$  and  $6 \mu\text{m}$  are closer to the value of  $\lambda_p/4$ , such that more bunch electrons can be confined in the created ion channel. Consequently, the collimation and emittance of the DLA-accelerated bunch can be improved. Comparing Figs. 2(a) with 3(b), the emittance  $\epsilon_{N,y}$  can be considerably reduced by increasing the bunch duration to  $\tau_b = 13$  fs and 20 fs with the same delay time  $\tau_d = 0$ . The bunch electrons can be more concentrated at the waveguide center, as shown in Fig. 3(c) at those longer bunch durations, which is attributed to the enhanced ion-focusing effect. In contrast to the trace space results obtained for short bunches, electrons concentrated in  $|y| \leq 5 \mu\text{m}$  in Fig. 3(b) can have a large value of  $\theta_y$  due to the increased transverse momentum  $P_y$  driven by the ion focusing force. Fig. 3(c) also shows that more electrons at the leading and trailing edges cannot be effectively accelerated/decelerated when the bunch duration becomes comparable to the laser pulse duration of  $\tau_p = 20$  fs. Therefore, the final energy spectra in Fig. 3(d) become more uniform with increased bunch duration  $\tau_b$ .

The finite diameter of the laser beam limits the size of the effective radial region and the efficiency of DLA because of the reduced axial field available to the off-axis

electrons [2]. On the other hand, the density modulation is enhanced as the off-axis electrons experience a stronger radial focusing/defocusing Lorentz force  $F_r \propto q_e E_r$ . To understand the effect of the electron bunch diameter on DLA, bunches with two diameters ( $w_b = 9 \mu\text{m}$  and  $15 \mu\text{m}$ ), fixed duration  $\tau_b = 6$  fs, and  $q_b = 5$  pC charge are injected. In both cases the bunches are assigned the same initial emittance  $\epsilon_{N,y} \approx 1\pi\text{-mm-mrad}$ , so that the divergence angles are  $\Delta\theta_y \approx 1.96$  mrad and  $1.177$  mrad for  $w_b = 9 \mu\text{m}$  and  $15 \mu\text{m}$ , respectively. Fig. 4(a) summarizes the variation of the bunch density during the entire propagation through the waveguide with  $w_b = 9 \mu\text{m}$ , in which the radial force  $F_r$  periodically focuses and defocuses the bunch electrons, depending on their injection phase with respect to the radial field  $E_r$ . At  $t = 3.5$  ps, densities of the microbunches reach their peak values, up to one order of magnitude higher than the injected peak density of  $n_{b0} = 1.78 \times 10^{17} \text{cm}^{-3}$ . The diameter of the microbunches is reduced to approximately  $2 \mu\text{m}$  as the electrostatic force is balanced by the radial force. However, microbunch density is reduced when the bunch arrives the exit of the waveguide due to the de-bunching effect arising from the axial velocity modulation of the bunch electron. Fig. 4(b) shows the change of emittance  $\epsilon_{N,y}$  when bunches of  $w_b = 9 \mu\text{m}$  and  $15 \mu\text{m}$  are injected. In both cases, the emittance  $\epsilon_{N,y}$  changes periodically and tends to increase as the bunch propagates through the waveguide. As shown in Fig. 4(c), electrons are significantly scattered because of the enhanced defocusing effect with the larger bunch size  $w_b = 9 \mu\text{m}$ . The DLA efficiency is reduced, as shown by the final energy spectra in Fig. 4(d), where a large fraction of the bunch electrons still have energies around the initial value of 40 MeV.

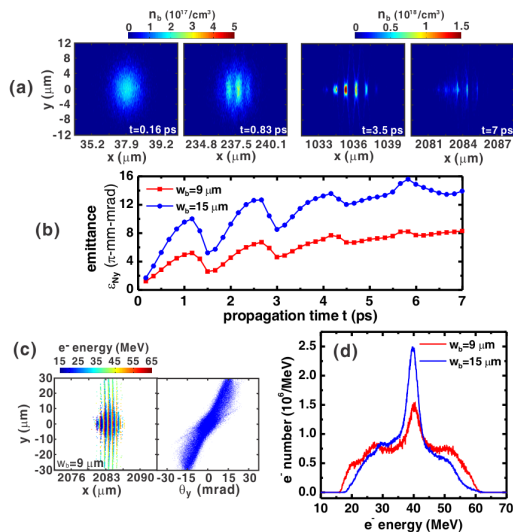


Figure 4: (a) Sampled 2-D bunch density variation over the electron propagation. (b) Bunch emittance  $\epsilon_{N,y}$  as a function of propagation time  $t$  for bunches with widths  $w_b = 9 \mu\text{m}$  and  $15 \mu\text{m}$ . (c) Final trace space and electron distributions for  $w_b = 9 \mu\text{m}$ . (d) Final energy spectra for bunches of  $w_b = 9 \mu\text{m}$  and  $15 \mu\text{m}$ .

## CONCLUSION

It can be concluded from the combined results that the injection of an electron bunch with a long bunch length (close to  $\lambda_p/4$ , referring to the low-density plasma region) and a small transverse size with respect to the laser pulse diameter is preferred for maintaining the favorable bunch transverse properties in DLA in a plasma waveguide.

## ACKNOWLEDGMENT

The authors wish to thank Prof. S.-H. Chen of National Central University in Taiwan for helpful discussions and providing the computational resources needed to conduct this work.

## REFERENCES

- [1] P. Serafim, IEEE Trans. Plasma Sci. **28**, 1155 (2000).
- [2] M.-W. Lin and I. Jovanovic, Phys. Plasmas **19**, 113104 (2012).
- [3] C. Nieter and J. R. Cary, J. Comput. Phys. **196**, 448 (2004).